The oligomerization of acetylene in hydrogen over Ni/SiO$_2$ catalysts: Product distribution and pathways

David L. Trimm [a], Irene O.Y. Liu [b], Noel W. Cant [c,*]

[a] *CSIRO Petroleum, Clayton South, Vic. 3169, Australia*
[b] *School of Chemical Sciences and Engineering, The University of New South Wales, Sydney, NSW 2052, Australia*
[c] *Department of Chemistry and Biomolecular Sciences, Macquarie University, NSW 2119, Australia*

ARTICLE INFO

ABSTRACT

The characteristics of nickel on silica catalysts for the reaction of acetylene in the presence of hydrogen in a flow system are investigated. Samples containing 2 wt% Ni are capable of complete acetylene conversion over a period of 5 h at 140 °C when using a 25% C$_2$H$_2$/75% H$_2$ feed. Ethylene and ethane account for approximately one-half of the acetylene converted with methane formation low. The remaining acetylene is converted to a multitude of oligomers with even-numbered ones typically three times as common as odd-numbered ones. The predominant C$_4$ and C$_5$ products are linear alkenes in a non-equilibrium distribution (1 > *cis*-2 > *trans*-2) followed by branched alkenes (isobutene and the three methylbutenes), alkanes and traces of dienes. A further major class in the C$_6$ fraction are 3-methyl branched products, such as *cis*- and *trans*-3-methyl-2-pentene and 3-methyl-1,3-pentadiene, which lack hydrogen atoms at the branch. The product distribution amongst higher oligomers appears to be similar based on the structures of the alkanes produced when Pt/SiO$_2$ is placed downstream of Ni/SiO$_2$. Aromatics are minor products—less than 3% of the acyclic products formed at each of carbon numbers 6, 7 and 8 and less than that of the corresponding cyclopentanes observed when the Pt/SiO$_2$ is present. Formation of all product classes, with the exception of those with a 2-methyl branch such as isobutene, can be rationalised in terms of chain growth initiated by addition of C$_2$ units to surface species established in surface science studies of acetylene adsorbed on nickel surfaces. Rearrangement is necessary for formation of the 3-methyl branched products.

1. Introduction

Hall et al. [1,2] have described the development of an integrated process for converting natural gas to liquid fuels via short residence time pyrolysis to acetylene and ethylene with subsequent oligomerization to produce liquid fuels. The associated patents [3–5] emphasise the direct conversion of acetylene over an acidic zeolite, but acetylene hydrogenation followed by ethylene oligomerization was stated to be preferable for commercial operation [2]. The acetylene oligomerization catalyst was not described in detail, but based on other work by one of the authors, it appears to be H-ZSM5 loaded with Ni, Pt or Pd [6]. The yields of liquid fuel were not stated but deactivation was a problem with activity falling very steeply after 3 h on stream despite a H$_2$/C$_2$H$_2$ ratio of 2.5. Such deactivation is characteristic of the reaction of acetylene over H-ZSM5 catalysts where aromatics are major products [7,8]. In the

case of Ni/ZSM5/Al$_2$O$_3$ at 350 °C, such deactivation can be largely prevented by co-feeding water but methane then makes up ~25% of the products while the >C$_5$ products are largely aromatic and restricted to a yield of ~30% [9].

Nickel has been known to be active for the oligomerization of acetylene at low temperature since the 1930s. Peters and Neumann [10] reported a yield of up to 60% vapours condensable on charcoal at 0 °C using nickel-iron catalysts and Sheridan [11] claimed 40–70% C$_4$$^+$ material, thought to be largely straight chain, over 20% nickel on pumice. More detailed studies by Antzus and Petrov [12,13] show that a multitude of branched oligomers can also form, particularly if Ni/pumice is passivated with ZnCl$_2$ or CoCl$_2$ [14,15]. Results reported in more recent studies are more divergent. Vasquez [16], using 13 wt% Ni/H-ZSM5-Al$_2$O$_3$, observed a liquid yield of ~6% with C$_3$$^+$ material comprising approximately one-half of the gaseous products over the temperature range 150–300 °C. However, Boudjahem et al. [17] claimed that benzene was the principal non-C$_2$ product for 1–5 wt% Ni/SiO$_2$ at temperatures below 150 °C.

In recent work the activity of catalysts of the type investigated by Vasquez [16] has been compared with systems containing less nickel and mounted on other supports [18]. All gave yields of

* Corresponding author.
E-mail addresses: David.Trimm@csiro.au (D.L. Trimm), iliu@unsw.edu.au (I.O.Y. Liu), noel.cant@mq.edu.au (N.W. Cant).

products in the C_4–C_{10} range of ∼40%, with nickel on silica showing the least deactivation. The aim of the present work was to explore acetylene oligomerization over low-loaded Ni/SiO$_2$ catalysts in detail, paying particular attention to carbon number and isomer distribution as clues to reaction pathways.

2. Experimental

Catalysts were tested in a flow system with samples located in a 6 mm ID Pyrex reactor mounted vertically so that liquid products drained into a lower receiver cooled to 0 °C. In some cases a second trap cooled to −78 °C was arranged downstream. Standard test conditions involved 200 mg of catalyst with a feed comprising 25% C_2H_2 in H_2 (Linde, 99.99%) at a combined flow rate of 50 cm^3 (STP)/min, a GHSV of ∼5000 h^{-1}. The acetylene was instrument grade from BOC (Australia) and contained ∼0.25% acetone when fed from the cylinder at room temperature. Trials showed that acetone was unreactive over nickel on silica under the conditions of acetylene oligomerization but ∼50% was hydrogenated to isopropanol in experiments with Pt/SiO$_2$ downstream as shown later in Fig. 6.

The methods used for product analysis were progressively refined during the study. The final version comprised parallel on-line analyses of untrapped vapours by two chromatographs, a MTI M200 chromatograph fitted with Poraplot U and molecular sieve (5 Å) columns, both at 60 °C, and a Shimadzu GC17A chromatograph with a 30 m by 0.53 mm AT-Q column (Alltech Corp.). The Poraplot U column provided analysis for all C_1, C_2 and C_3 products while the molecular sieve column eluted hydrogen, isobutane and then isobutene, all retained minimally by the sieve, followed by methane. The AT-Q column, programmed from 60 to 130 °C at 6.5 °C/min and then to 240 °C at 10 °C/min, produced fully resolved peaks for C_2, C_3 and most C_4 compounds plus two incompletely resolved envelopes attributable to C_5 and $\geq C_6$ vapour fractions.

Trapped compounds in the range C_4 to above C_{20} were analysed off-line using a Shimadzu GC–MS QP-5050 fitted with a 60 m × 0.25 mm Rtx-1 column (Restek) which was programmed from 50 to 150 °C at 5 °C/min, from 150 to 250 °C at 10 °C/min and then to 330 °C at 30 °C/min. In cases where isomeric compounds exhibited very similar mass spectra, the identifications also used elution order and calculated Kovats indices compared with values from several literature sources, principally those in the ASTM standard for the analysis of reformulated gasoline [19], those of Sojak et al. [20,21] for the C_5–C_8 alkenes in the products of fluid catalytic cracking and of Hayes and Pitzer [22] for shale and petroleum derived jet fuels. The identification of individual isomeric dienes was least certain since the available Kovats indices were largely confined to old data for packed columns operated isothermally [23]. The identification of two C_6 dienes of particular interest (cis- and trans-3-methyl-1,3-pentadiene) was confirmed by measurements on a mixture of the two sourced from Aldrich Chemical Company. Comparison of the proton NMR spectrum of this sample with data reported by Altbach and Fitzpatrick [24] indicated that it contained ∼72 mol% of the trans-isomer and 28 mol% of the cis. Chromatography on the Rtx-1 column showed two peaks with the smaller one eluting first. Their retention times and mass spectra were close matches to those for two peaks in the chromatogram of liquid products as shown in Fig. 7.

Individual compounds up to C_{10} were quantified more exactly than possible with the GC–MS by FID-GC analysis on another Rtx-1 column, identical to that used in the GC–MS, but installed in the GC17A chromatograph also used for on-line gas analysis. This column was operated identically to that in the GC–MS but the program was terminated at 240 °C to avoid damage to the AT-Q column present in the oven. NMR spectra of trapped material were obtained from ∼15% solutions in CDCl$_3$ measured with a Bruker DPX300 spectrometer operated at 300 MHz for ^{1}H and 125.03 MHz for ^{13}C.

Most of the catalysts were made by standard incipient wetness impregnation of Davison grade 62 silica gel (surface area 285 m^2/g, particle size 75–250 μm) using solutions of Ni(NO$_3$)$_2$, Pt(NH$_3$)$_4$(NO$_3$)$_2$, Pd(NO$_3$)$_2$ and Rh(NO$_3$)$_2$ with concentrations set so that the complete uptake obtained gave a metal content of 2.0 wt%. Nickel supported on silica of this type carries the designation (H). Survey experiments were also carried out with a 13 wt% Ni catalyst made using the same support and with two other catalysts, designated 2% Ni/SiO$_2$(M) and 2% Ni/SiO$_2$(L), made in the same way with a loading of 2% but using silicas of lower areas, namely Davison type SMR-7 (100 m^2/g, crushed and sieved to 70–200 μm) and Davicat type SP-550-10010 (24 m^2/g, average particle size 100 μm), respectively. All preparations were dried at 120 °C and calcined in air at 450 °C. Individual samples were loaded into the reactor and reduced in pure H$_2$ according to a set program (ramp to 230 °C, hold for 30 min, ramp to 450 °C, hold 180 min, cool to reaction temperature in H$_2$).

TPR and CO-uptake measurements were carried out on 100 or 200 mg samples in a U-tube Pyrex reactor using an in-house flow system equipped with a quadrupole mass spectrometer (Balzers Thermostar GSD 301T). The samples were reduced in a 1% H$_2$/2% Ar/He stream at 40 cm^3/min on a 3 °C/min ramp to the standard reduction temperature of 450 °C and left there for 2 h. After cooling to near room temperature in He they were exposed to a flow of 2% CO/2% Ar/He. The amount of CO taken up was determined by integration of the normalised difference between the near parallel breakthrough curves for Ar ($m/z = 40$) and CO ($m/z = 28$ or 12) and corrected for a small amount of adsorption on the silica.

Powder X-ray diffraction measurements (XRD) were carried out using a Philips PW1830 powder diffractometer on samples that had been reduced according to the procedure used prior to catalytic measurements and then passivated by slow exposure to air. Transmission electron microscopy (TEM) measurements were carried out using a Tecnai 12 microscope on samples pretreated in the same way, suspended in ethanol by vortexing and then applied to 400 mesh carbon-coated grids.

3. Results

3.1. Catalyst characterization

TEM measurements on the 2 and 13% Ni/SiO$_2$(H) catalysts showed rounded nickel particles with mean size of 8.99 nm (for 217 particles) and 11.4 nm (for 130 particles), respectively. The corresponding estimates derived from XRD line widths using the Scherrer equation were 9.0 nm (from the (1 1 1) reflection peak alone) and 10.2 nm (average for five reflections), respectively.

Both samples showed at single peak during H$_2$-TPR to 450 °C with the maximum at 370 °C as expected for the reduction of a separate NiO phase [25]. The sensitivity of the mass spectrometer used was insufficient to allow an accurate determination of the extent of reduction for the 2% Ni/SiO$_2$(H) sample but it was 84% for the 13% Ni/SiO$_2$(H) sample. CO uptake measurements on the 2% sample gave a nickel surface area of 1.1 m^2/g(catalyst) assuming a CO/Ni(surface) ratio of unity with each Ni atom corresponding to 6.5×10^{-20} m^2. If the sample had been reduced to the same extent as the 13 wt% one then the measured area would correspond to a dispersion of ∼8.6% and a uniform sphere particle size of ∼10 nm, in good agreement with the XRD and TEM measurements. The particle size estimates are in line with the rather wide range of values reported in the literature for Ni/SiO$_2$ prepared by nitrate impreg-
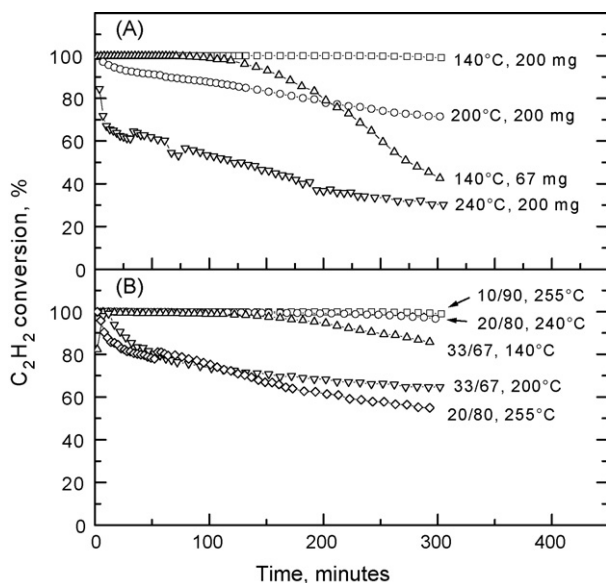
Fig. 1. Acetylene conversion version time on stream for reaction over 2 % Ni/SiO₂(H). (A) Effect of temperature and catalyst weight using the standard feed comprising 25% C_2H_2/75% H_2 at 50 cm³/min. (B) Effect of feed composition (shown as X% C_2H_2/Y% H_2) when using 200 mg of catalyst throughout.

Fig. 2. Carbon number distribution for reaction over 200 mg of 2% Ni/SiO₂(H) at 140 °C using the standard feed (25% C_2H_2/75% H_2 at 50 cm³/min) on successive days with overnight treatment in 5% H_2/He in between. The liquid product was collected at 0 °C as a single fraction over the 2-day experiment and has been prorated over the ~10 h of reaction assuming a constant production rate.

nation and calcination, e.g. 16 nm for 1.7 wt% Ni [26], 10.7 nm for 8.8 wt% Ni [25,26] and 10 nm for 8 wt% Ni [27].

XRD measurements on the Pt/SiO₂(H), Pd/SiO₂(H) and Rh/SiO₂(H) catalysts indicated particle sizes of ~14, ~23 and ~4.3 nm, respectively, calculated as the average of values derived from the widths of the (1 1 1) and (2 0 0) reflection peaks for the Pt and Pd-containing samples and the (1 1 1) peak alone for the Rh one.

3.2. General reaction characteristics

Fig. 1 shows acetylene conversion versus time for samples of the 2% Ni/SiO₂(H) catalyst, each used only once, under survey conditions encompassing temperature, feed composition and GHSV. Rates of deactivation were very dependent on temperature and composition. Under standard conditions (25% C_2H_2, 75% H_2, 200 mg, 50 cm³/min total flow, GHSV ~ 5000 h⁻¹), acetylene conversion was complete for 5 h at 140 °C, but deactivation was significant at 200 °C and much more pronounced at 240 °C (Fig. 1A). Deactivation became noticeable even at 140 °C when the mass of catalyst was reduced to 67 mg (GHSV ~ 15,000 h⁻¹). Increasing the concentration of C_2H_2 from 25 to 33% also induced deactivation at 140 °C (13% over 5 h) and increased it at 200 °C (Fig. 1B). Conversely, decreasing C_2H_2 was beneficial, with little deactivation at 240 °C when using a 20% C_2H_2/80% H_2 feed or at 255 °C when using 10% C_2H_2/90% H_2.

In survey experiments at 200 °C the 13% Ni/SiO₂(H) catalyst behaved similarly to the 2% catalyst but with somewhat less deactivation. The two catalysts based on silicas with lower area, Ni/SiO₂(M) and Ni/SiO₂(L) also showed marginally slower deactivation than 2% Ni/SiO₂(H) at 200 °C but similar behaviour when tested at 140 °C (with losses in conversions of 8 and 19%, respectively after 5 h using a 33% C_2H_2/67% H_2 feed). The results that follow are all for 2% Ni/SiO₂(H) catalyst which was the easiest to prepare and handle in multi-gram amounts. It will be referred to as simply Ni/SiO₂ in the text from now on.

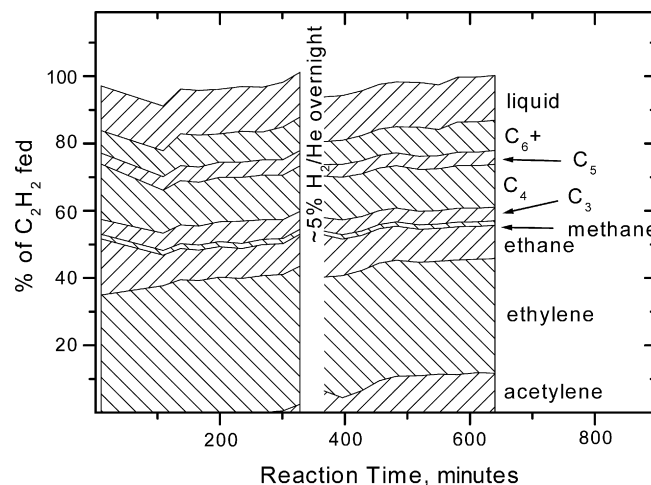Fig. 2 shows the composition of the exit gas for an experiment in which a single sample of Ni/SiO₂ was tested in the standard feed over two successive 5-h periods with an overnight exposure to 5% H_2/He in between. In this case breakthrough of C_2H_2 started near the end of the first 5-h period, and increased in the initial stages of the second 5 h before stabilising with ~15% of the input acetylene unreacted.

Of the gaseous products, ethylene and ethane in the ratio of ~3:1 accounted for almost 50% of the C_2H_2 reacted, followed by uncondensed oligomers with an even number of carbon atoms, C_4 (13%) and C_6 (9%). Methane formation was low (~1.5%) but significant amounts of higher odd-numbered compounds, C_3 and C_5, were present. Liquid condensed at 0 °C comprised approximately 13% of the acetylene converted. This liquid was pale yellow-green but a few droplets of a somewhat darker more viscous material were also retained on the inner walls of the Pyrex reactor below the catalyst. In overall terms, liquid and gaseous phases combined, the yield of C_5+ products was ~27% during the period of complete acetylene conversion.

GC–MS and FID-GC analyses of the liquid trapped in the receiver below the reactor showed several hundred peaks largely attributable to isomeric monolefins (internal, branched, *cis-* and *trans-*), with a broad envelope of unresolved compounds underneath. Proton and ¹³C NMR spectra (available from the authors) showed a predominance of saturated CH_3 and CH_2 groups, with a significant fraction attached to carbon-carbon double bonds. There was some evidence for small amounts for dienes and aromatics but acetylenic groups were completely absent. The possibility of simplifying the complex mixture of unsaturates by hydrogenation to alkanes without undesirable side reactions was examined as follows.

3.3. Characteristics of Pt/SiO₂, Pd/SiO₂ and Rh/SiO₂ catalysts

Fig. 3 shows the characteristics of the three metals (all supported on SiO₂(H)) for reaction of the standard 25% C_2H_2/75% H_2 mixture. All three metals achieved complete acetylene conversion for the full 5-h period at 140 °C with Pt/SiO₂ exhibiting the highest selectivity to ethane (>95%), followed by Pd/SiO₂ (~90%), and with C_4 production highest on Rh/SiO₂ (~20%). Likewise Rh/SiO₂ gave the highest yields of C_6 products (~5% of the C_2H_2 fed versus 3% for Pd/SiO₂ and 2% for Pt/SiO₂). The difference was even greater in tests carried out at 200 °C (not shown). Again Pt/SiO₂ achieved complete conversion over the full 5 h with ethane comprising >95% of the products but the other two catalysts were found to deactivate. With Pd/SiO₂,
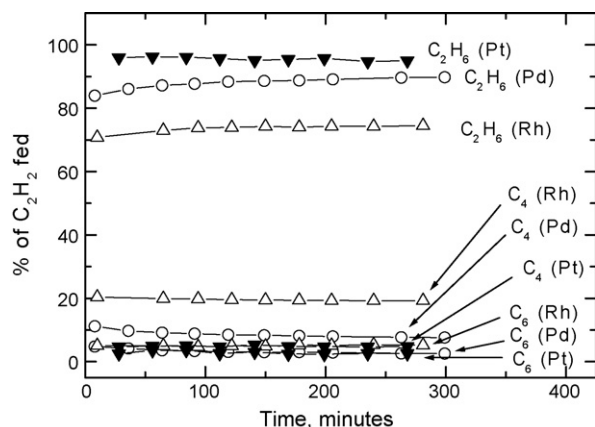
Fig. 3. Product distributions for reactions over 200 mg of Pt, Pd and Rh supported on $SiO_2(H)$ at 140 °C using the standard feed comprising 25% C_2H_2/75% H_2 at 50 cm³/min.

oligomer formation was less at 200 °C than at 140 °C, but ethylene emerged in addition to ethane after ~1 h and reached 23% after 5 h. The extent of oligomer formation using Rh/SiO_2 at 200 °C was similar to that at 140 °C but C_2H_4 comprised 50% of the acetylene reacted from the beginning of reaction. Unreacted C_2H_2 emerged after a few minutes and rose to 35% of that in the feed after 5 h while C_2H_4 declined to 38%. Thus Pt/SiO_2 was chosen as the most suitable catalyst for downstream hydrogenation.

Palladium catalysts in particular are normally regarded as having high selectivity for the hydrogenation of acetylene to ethylene rather than ethane [28]. The temperatures used here are higher than is usual, and contact times are also longer, leading to a situation in which acetylene is completely converted to ethylene in the first part of the catalyst bed. High conversion of ethylene to ethane is then possible during passage through the remainder of the bed. The pronounced difference between the three metals in terms of oligomer formation, seen in Fig. 3, has not been reported previously. Bond [28] lists values near 25% for all three metals taken from work carried out in static systems.

3.4. Gaseous C_3 and C_4 products using Ni/SiO_2 with and without Pt/SiO_2 downstream

Fig. 4A shows the distribution amongst gaseous C_3 and C_4 products when Ni/SiO_2 was used alone at 140 °C. As for the C_2 products in Fig. 2, the concentrations of C_3 and C_4 alkenes were several times those of the corresponding alkane concentrations. The distribution amongst the linear alkenes (1-butene ≥ *cis*-2 ≫ *trans*-2) was very different from the equilibrium ratio at 140 °C (1-butene:*cis*-2:*trans*-2 ≈ 1:3.1:6.4 [29]). The AT-Q column was unable to resolve 1,3-butadiene but parallel analyses on another chromatograph fitted with a PLOT-alumina column during one run showed that its concentration was at most 2.5% of all C_4 products. The possibility that the butenes observed with Ni/SiO_2 were formed via hydrogenation of 1,3-butadiene as a gaseous intermediate could be excluded since such a reaction would be expected to result in a *trans*-2:*cis*-2 ratio of at least 2 [30,31].

In experiments with 200 mg of Pt/SiO_2 downstream of 200 mg of Ni/SiO_2, the 35% ethylene formed by reaction of the standard C_2H_2/H_2 mixture on the latter alone was almost completely hydrogenated to ethane as expected. The C_3 and C_4 fractions produced on Ni/SiO_2 were also hydrogenated to a large extent (Fig. 4B) but the degree varied considerably from compound to compound. The concentrations of propene and isobutene were reduced to negligible values and have been omitted for the sake of clarity. The concen-
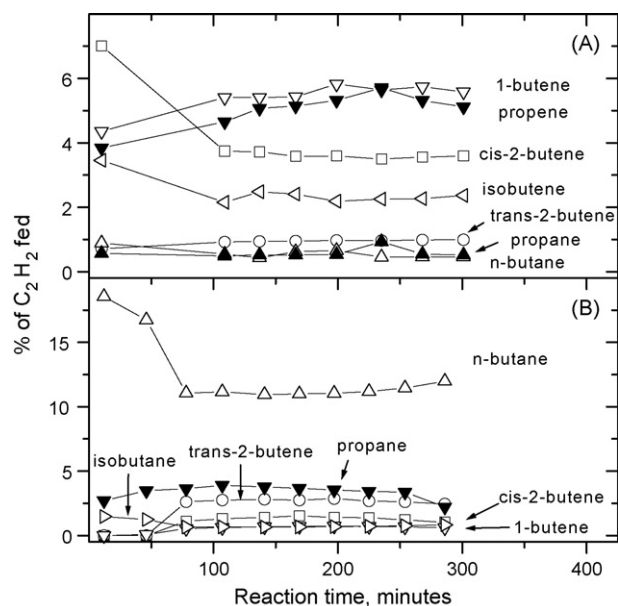

Fig. 4. On-line analyses of C_3 and C_4 vapour products for reaction at 140 °C using the standard feed (25% C_2H_2/75% H_2 at 50 cm³/min). (A) 200 mg 2% $Ni/SiO_2(H)$; (B) 200 mg 2% $Ni/SiO_2(H)$ with 200 mg of Pt/SiO_2 downstream.

trations of 1-butene and *cis*-2-butene were also much reduced, but bearing in mind the difference in scale between Fig. 4A and B, the concentration of *trans*-2-butene actually doubled. This is possible only if the rates of both double-bond migration and *cis–trans* interconversion to form the thermodynamically more favoured *trans*-isomer were considerably faster than that of hydrogenation to *n*-butane. Indeed, the 1-butene:*cis*-2-butene:*trans*-2-butene ratio, averaged over the period from 75 to 250 min of reaction, was ~1:2:4 which approaches the equilibrium ratio of 1:3.1:6.4 at 140 °C [29].

3.5. Composition of the liquid trapped at 0 °C

The liquid trapped at 0 °C with Pt/SiO_2 downstream was colourless, unlike the pale yellow-green product formed when using Ni/SiO_2 alone and, at the end of the experiment, the reactor walls downstream were free of the droplets of darker material formed with Ni/SiO_2 alone. Fig. 5 shows the FID chromatograms of the liquid fractions produced by Ni/SiO_2 and by Ni/SiO_2 followed by Pt/SiO_2. As expected, the composition was much simpler with the Pt/SiO_2 present, with easily identifiable peaks due to *n*-alkanes. They alternate in peak height with odd-numbered hydrocarbons being approximately one-half that of next higher even-numbered one.

As well as simplifying the product mixture, the presence of Pt/SiO_2 seemed to result in a slightly higher proportion of lighter products. The fraction of molecules with carbon number above 10, obtained by integration above the dotted baseline for retention times beyond 20 min, was 0.53 with Pt/SiO_2 present compared with 0.63 when Ni/SiO_2 was used alone. There are two possible explanations. One is that long chain molecules were fragmented as well as hydrogenated on the Pt/SiO_2. That seems unlikely at a temperature of 140 °C. An alternative possibility is that the primary reaction on Ni/SiO_2 produced some highly conjugated reactive compounds that can undergo secondary condensation reactions downstream. If the highly reactive compounds were immediately hydrogenated on Pt/SiO_2 then the final liquid product would be lighter. The formation of a colourless product, and the absence of droplets of viscous
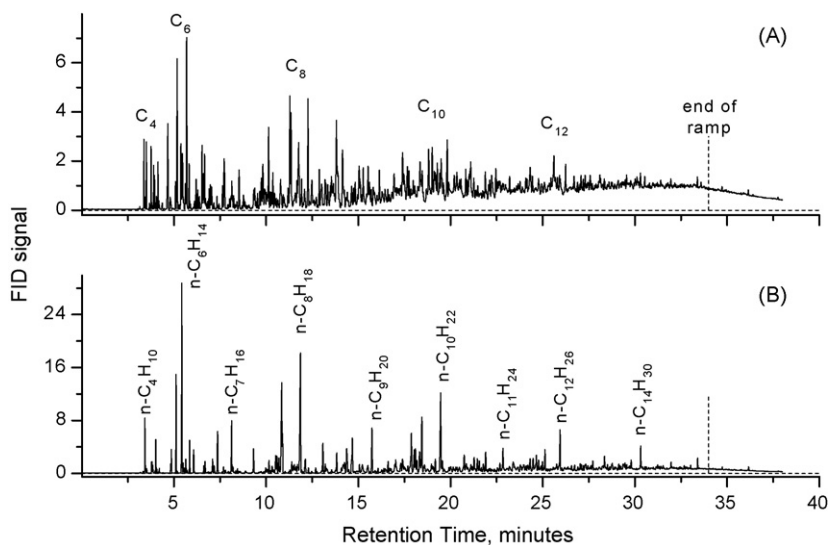
Fig. 5. Complete FID chromatograms of the liquid products collected over 5 h of reaction at 140 °C with the standard feed (25% C_2H_2/75% H_2 at 50 cm³/min). (A) 200 mg 2% Ni/SiO₂(H); (B) 200 mg 2% Ni/SiO₂(H) with 200 mg of Pt/SiO₂ downstream.

material below the catalyst when Pt/SiO₂ was present, is consistent with such an explanation.

The relative intensities of peaks in Fig. 5A and B, and those in Figs. 6–8 which follow, are biased away from products with low-carbon number. This is because the efficiency with which the latter were collected at 0 °C was much lower—55 to 80% for C_8 compounds but <30% for C_6, about 1% for *n*-butane and less still for isobutane, the lowest boiling C_4.

3.6. C_4 and C_5 products in the liquid phase

Fig. 6 shows the C_4/C_5 region of the chromatograms of the liquid products. As expected, the distribution amongst the linear C_4 alkenes matched that exhibited for the corresponding gaseous fractions in Fig. 4. 1-Butene and *cis*-2-butene, the principal products on Ni/SiO₂ alone, were largely hydrogenated to *n*-butane when Pt/SiO₂ was downstream with the thermodynamically more stable *trans*-2-butene, produced by isomerisation of the 1- and *cis*-2-isomers,

remaining in the largest amount. Isobutene cannot be seen in Fig. 6A as it lies beneath the 1-butene peak but hydrogenation on Pt/SiO₂ resulted in the appearance of a small amount of isobutane in Fig. 6B as expected.

A similar pattern was evident for the C_5 products. 1-Pentene and *cis*-2-pentene predominated over the thermodynamically more stable *trans*-2-pentene in the products using Ni/SiO₂ alone. Rapid isomerisation on Pt/SiO₂ prior to hydrogenation resulted in a preponderance of the more stable *trans*-2-pentene remaining after hydrogenation in the sequential system. Likewise, Ni/SiO₂ produced all three branched chain alkenes, 3-methyl-1-butene, 2-methyl-1-butene and 2-methyl-2-butene, in the approximate ratio, 1:5:1.4, which was well away from the 1:24:96 estimated for equilibrium at 140 °C using the data in standard sources [32,33]. As expected, Pt/SiO₂-catalysed hydrogenation of the mixture yielded 2-methylpentane with only the thermodynamically most preferred branched isomer, 2-methyl-2-butene, and the second most preferred one (2-methyl-1-butene) remaining in observable amounts.
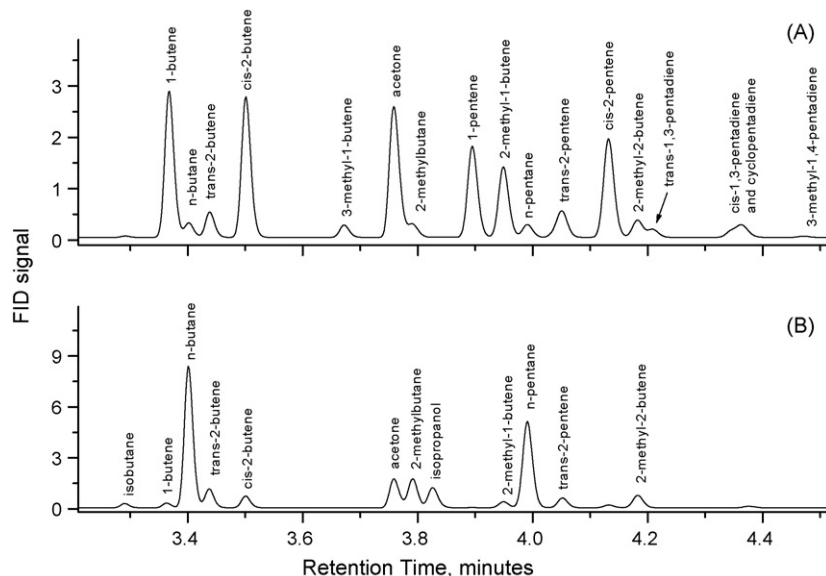

Fig. 6. C_4–C_5 region of the FID chromatograms of the liquid products collected over 5 h of reaction at 140 °C using the standard feed (25% C_2H_2/75% H_2 at 50 cm³/min). (A) 200 mg 2% Ni/SiO₂(H); (B) 200 mg 2% Ni/SiO₂(H) with 200 mg of Pt/SiO₂ downstream.
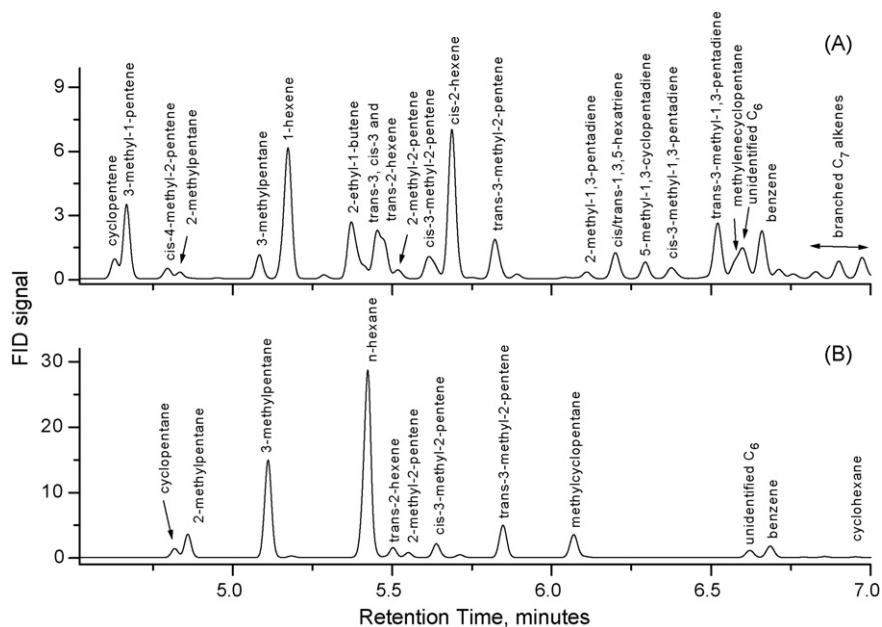
Fig. 7. C_6 region of the FID chromatograms of the liquid products collected over 5 h of reaction at 140 °C using the standard feed (25% C_2H_2/75% H_2 at 50 cm³/min). (A) 200 mg 2% Ni/SiO₂(H); (B) 200 mg 2% Ni/SiO₂(H) with 200 mg of Pt/SiO₂ downstream.

It is notable that Ni/SiO₂ also gave rise to small amounts of cis- and trans-1,3-pentadiene (which largely disappeared during subsequent reaction on Pt/SiO₂), of cyclopentadiene and also of cyclopentene which eluted close to the first of the C_6 products as shown later in Fig. 7A. As would be expected, hydrogenation on Pt/SiO₂ converted the cyclic C_5 unsaturates to cyclopentane (see Fig. 7B later).

3.7. Liquid C_6 products

Although this portion of the liquid products accounted for <2% of the acetylene reacted, it is particularly informative in terms of the pathways through which oligomers are constructed.

Amongst the linear hexenes, cis-2- and 1-hexene dominated in the products using Ni/SiO₂ (Fig. 7A) with lesser concentrations of 3-hexenes or of trans-2-hexene, the most stable linear hexene [34]. However, the trans-2-hexene was left in the largest amount after the near complete hydrogenation of the linear hexenes to n-hexane on Pt/SiO₂ (Fig. 7B), as expected if the latter was active for double-bond shift. The four most prominent branched alkenes formed with Ni/SiO₂ alone were 3-methyl-1-pentene, 2-ethyl-1-butene and cis- and trans-3-methyl-2-pentene. All have backbones such that 3-methylpentane became their complete hydrogenation product on Pt/SiO₂. Correspondingly, the less significant methyl-branched products of reaction on Ni/SiO₂ (2-methyl-1-pentene, 4-methyl-1-pentene, cis- and trans-4-methyl-2-pentene and 2-
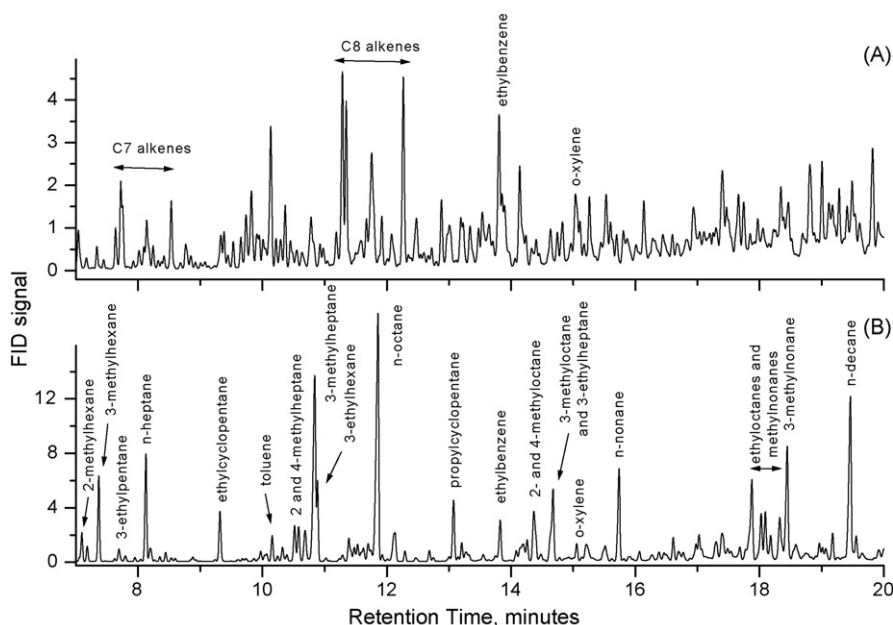

Fig. 8. C_7–C_{10} region of the FID chromatograms of the liquid products collected over 5 h of reaction at 140 °C using the standard feed (25% C_2H_2/75% H_2 at 50 cm³/min). (A) 200 mg 2% Ni/SiO₂(H); (B) 200 mg 2% Ni/SiO₂(H) with 200 mg of Pt/SiO₂ downstream.

Table 1
C_2H_2 (in ppm) converted to liquid C_6 products for Ni/SiO_2 alone and for $Ni/SiO_2 + Pt/SiO_2$[a]

Name	Class[b]	Elution time (min)	At 140 °C		At 200 °C		Collection[c] efficiency (%)
			Ni only	Ni + Pt	Ni only	Ni + Pt	
3-Methyl-1-pentene	bI	4.67	101	<4	74	9	6.8
cis-4-Methyl-2-pentene	bII	4.79	16	47	11	53	8.2
2-Methylpentane	bII	4.86	10	119	8	67	9.4
3-Methylpentane	bI	5.11	34	510	23	265	10.5
1-Hexene	L	5.17	206	9	186	45	10.7
2-Ethyl-1-butene	bI	5.37	115	<4	93	<4	11.2
n-Hexane	L	5.42	<4	1055	<4	661	13.3
trans-2-, *cis*-3-, *trans*-3-Hexene	L	5.45	115	56	96	198	12.3
2-Methyl-2-pentene	bII	5.52	13	<4	26	22	12.3
cis-3-Methyl-2-pentene	bI	5.61	46	77	30	80	12.4
cis–*cis*-2-Hexene	L	5.69	225	16	190	133	12.9
trans-3-Methyl-2-pentene	bI	5.82	65	180	56	137	13.7
Methylcyclopentane	cC5	6.07	<4	140	<4	86	14.4
2-Methyl-1,3-pentadiene	bII	6.11	12	<4	13	<4	16.6
cis/trans-1,3,5-Hexatriene	L	6.20	42	<4	63	<4	18.2
5-Methyl-1,3-cyclopentadiene	cC5	6.29	26	<4	39	<4	18.1
trans-3-Methyl-1,3-pentadiene	BI	6.37	20	<4	22	<4	16.5
cis-3-Methyl-1,3-pentadiene	bI	6.52	91	<4	105	<4	17.1
Benzene	cC6	6.66	77	69	136	89	24.4
Yield in condensed liquid as a % of C_2H_2 fed			0.48	0.91	0.47	0.74	

[a] *Feed*: 25% C_2H_2 (i.e. 250,000 ppm)/75% H_2 at total flow rate of 50 cm^3 (STP)/min over 200 mg Ni/SiO_2 alone, or over 200 mg Ni/SiO_2 with 200 mg Pt/SiO_2 downstream.

[b] L, linear product; bI and bII, branched products (see text for distinction); cC5, five-membered ring product; cC6, six-membered ring product.

[c] Estimated for reaction over Ni/SiO_2 alone at 140 °C. Values for alkanes and benzene are calculated using the vapour pressure data in Ref. [33] assuming that the vapour and liquid phases are fully equilibrated and Raoult's law is obeyed. Values for the unsaturates are estimated from that for the alkanes based on logarithmic interpolation against boiling points or, in cases where none was available, then against gas chromatographic retention time.

methyl-2-pentene) have 2-methylpentane as their hydrogenation product on Pt/SiO_2.

The C_6 oligomerization products of reaction over Ni/SiO_2 alone included at least eight di- and tri-unsaturates eluting between 6.15 and 6.7 min (Fig. 7A). Three of these, benzene and *cis*- and *trans*-3-methyl-1,3-pentadiene could be identified with certainty by comparison against chromatograms of authentic samples. The others were somewhat less certain with one peak unidentified. Six of the eight compounds underwent complete hydrogenation on Pt/SiO_2. The expected products for four of them (1,3,5-hexatriene and the three methylpentadienes) corresponded to C_6 alkenes already present in the product spectrum for reaction over Ni/SiO_2. The one unique hydrogenation product was methylcyclopentane, for which 5-methyl-1,3-cyclopentadiene and methylenecyclopentane are feasible progenitors. Benzene and the unidentified C_6 compound largely resisted hydrogenation. (Note the difference in *y*-scales between Fig. 7A and B and the low concentration of cyclohexane observed when Pt/SiO_2 was downstream.)

One aspect of the C_6 product distribution over Ni/SiO_2 alone is rather noteworthy. The *trans/cis* ratio in both 3-methyl-1,3-pentadiene and 3-methyl-2-pentene (which have the same carbon framework if the terminal double bond in the diene is excluded) was considerably greater than unity, and hence as expected for equilibrium if the general expectation that *trans*-isomers are thermodynamically more stable than *cis*-isomers applies. This was in contrast to the situation with the linear C_4, C_5 and C_6 alkenes, which were clearly not formed at equilibrium since the less stable 1- and *cis*-2-isomers dominate. Unfortunately there are no experimental data for the equilibrium *trans/cis* ratio in the above 3-methyl branched alkene and diene pairs which enable this distinction to be made with certainty. The calculations of Kilpatrick et al. [34], which rely on group correlations, give a *trans/cis* ratio of 1.5 for the 3-methyl-2-pentenes at 140 °C and this is in line with general expectations. However, estimates using Benson's group additivity method, as implemented on the NIST website [35], suggested that *cis*-3-methyl-1,3-methylpentadiene should be more stable than the *trans* counterpart.

Table 1 compares the amounts of the individual C_6 liquid products formed during reaction at 140 °C with the corresponding data for matching experiments at 200 °C. The products using Ni/SiO_2 alone at the higher temperature were less saturated with more benzene, dienes and trienes but less monoalkenes. The hydrogenation activity of Pt/SiO_2 was much reduced at 200 °C with considerably higher concentrations of the linear hexenes remaining than when 140 °C was used. It will be noted that, at both temperatures the total conversion to all listed C_6 compounds was greater when Pt/SiO_2 was downstream. To some extent this arose from variations in collection efficiency (final column Table 1) and because contributions from minor C_6 products not listed in Table 1 were greater when Ni/SiO_2 was used alone. However it is also a reflection of the earlier observation that the overall product distribution was lighter with Pt/SiO_2 present, possibly due to the hydrogenation of reactive compounds that would otherwise condense to higher molecular weight compounds.

The vapour compositions and collection efficiencies in Table 1 can be combined to provide estimates for total yields (i.e. the sum of that in the liquid condensed in the trap and the vapour passing through it). Table 2 summarises these estimates subdivided according to the arrangement of carbon atoms in the backbone.

Table 2
Approximate total yields for C_6 product classes as a % of C_2H_2 fed[a]

Product class	At 140 °C		At 200 °C	
	Ni only	Ni + Pt	Ni only	Ni + Pt
Linear (L)	1.9	3.4	1.7	3.2
Branched I (bI)	1.7	2.7	1.4	1.7
Branched II (bII)	0.2	0.5	0.2	0.4
Cyclic C5 (cC5)	0.06	0.4	0.1	0.2
Cyclic C6 (cC6)	0.1	0.1	0.2	0.15
Total	4.0	7.1	3.6	5.7
% L + bI	91	86	86	86

[a] For vapour and liquid phases combined based on liquid analyses and collection efficiencies shown in Table 1.

There are five classes, linear (L in Table 1), 5-membered ring compounds (cC5), 6-membered ring compounds (cC6), and two types of branched structures, bI and bII. Class bI comprises those compounds with a backbone that can be created by direct combination of surface C_2 units if one neglects, for the time being, the number of hydrogen atoms carried by each carbon. If two such C_2 units were to link end to end then they would form a surface C_4 intermediate with butane, butadiene and linear butenes as possible termination products:

$$C^*-C^* + C^*-C^* \rightarrow C^*-C^*-C^*-C^* \rightarrow C_4H_6, \quad C_4H_8, \quad C_4H_{10}$$
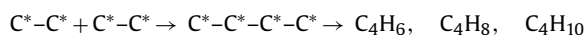
Addition of another C_2 unit to an end carbon of the C_4 intermediate would then produce a linear C_6 intermediate leading to hexane, linear hexenes, etc.

$$C^*-C^*-C^*-C^* + C^*-C^* \rightarrow C^*-C^*-C^*-C^*-C^*-C^*$$
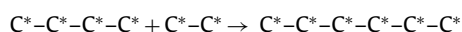
while addition at a central carbon would give a branched intermediate

$$C^*C^*C^*C^* + C^*C^* \rightarrow \begin{array}{c} C^*C^*C^*C^* \\ | \\ C^*C^* \end{array}$$
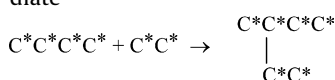
with a carbon backbone the same as that in bI type molecules, e.g. 3-methylpentane, 2-ethyl-1-butene, 3-methyl-1,3-pentadiene, etc. Branched C_6 products that cannot be produced through these direct C_2 addition processes (e.g. 2-methylpentane and 4-methyl-1-pentene) are designated class bII.

Table 3
Extents of hydrogenation in % for C_6 product classes[a]

Product class	At 140 °C		At 200 °C	
	Ni only	Ni + Pt	Ni only	Ni + Pt
Linear (L)	<2	92	<2	62
Branched I (bI)	7	71	6	59
Branched II (bII)	22	>90	17	46
Cyclic C_5 (cC5)	<10	>90	<10	>90
Cyclic C_6 (cC6)	<10	<10	<10	<10

[a] Calculated as alkanes/(alkanes + alkenes plus dienes and trienes) using data in Table 1.

It is apparent from Table 2 that compounds of types L and bI dominated, making up 80–90% of all C_6 products with both catalyst systems. Benzene was less that 2% of the total, considerably less that that of the methylcyclopentane present after hydrogenation. As shown in Table 3, the extent of hydrogenation also depends on structure especially when Pt/SiO$_2$ is downstream. It is much higher for linear and cyclic C_5 compounds, rather less for branched compounds and negligible for the cyclic C_6 molecules (i.e. benzene).

3.8. Liquid C_7–C_{10} products

It was not possible to identify the multitude of C_7–C_{10} alkenes produced over Ni/SiO$_2$ (Fig. 8A) alone with any certainty due to peak overlap and similarities in mass spectra. However the col-

Table 4
C_4–C_{10} alkanes and aromatics in liquid trapped with Pt/SiO$_2$ downstream of Ni/SiO$_2$[a]

Compound	Class	Elution time (min)	C_2H_2 used (ppm)		Collection[b] efficiency (%)
			140 °C	200 °C	
n-Butane	L	3.42	198	76	0.8
2-Methylbutane	bI	3.82	45	25	2.6
n-Pentane	L	4.02	137	101	3.6
Cyclopentane	cC5	4.82	47	53	6.1
2-Methylpentane	bII	4.86	119	67	9.4
3-Methylpentane	bI	5.11	510	265	10.5
n-Hexane	L	5.42	1055	661	13.3
Methylcyclopentane	cC5	6.07	140	86	14.4
Benzene	cC6	6.68	69	89	24.4
2-Methylhexane	bI*	7.09	100	126	27.8
3-Methylhexane	bI	7.37	267	208	29.3
3-Ethylpentane	bI	7.69	49	84	30.5
n-Heptane	L	8.12	351	297	36.6
Ethylcyclopentane	cC5	9.31	185	143	39.3
Toluene	cC6	10.16	90	181	48.7
2-Methylheptane	bII	10.52	138	95	57.4
4-Methylheptane	bII	10.58	131	95	57.5
3-Methylheptane	bI	10.84	866	512	58.8
3-Ethylhexane	bI	10.88	229	196	58.0
n-Octane	L	11.86	1162	867	67.2
Propylcyclopentane	cC5	13.08	230	166	71.5
Ethylbenzene	cC6	13.82	169	291	75.0
2- and 4-Methyloctane	bI*	14.37	269	239	80.0
3-Methyloctane and 3-ethylheptane	bI	14.68	366	298	80.5
o-Xylene	cC6	15.06	69	102	77.6
n-Nonane	L	15.74	351	312	86.3
4-Ethyloctane	bI	17.88	424	275	91.2
5-Methylnonane	bI*	18.03	220	170	91.5
Unidentified C_{10} alkane	–	18.09	201	195	91.8
2-Methylnonane	bII	18.18	114	100	92.1
3-Ethyloctane	bI	18.32	244	180	92.3
3-Methylnonane	bI	18.44	507	315	92.5
n-Decane	L	19.46	770	581	94.8
Yield in condensed liquid as a % of C_2H_2 fed			3.9	3.0	

[a] Feed: 25% C_2H_2 (i.e. 250,000 ppm)/75% H_2 at total flow rate of 50 cm^3 (STP)/min over 200 mg Ni/SiO$_2$ alone, or over 200 mg Ni/SiO$_2$ with 200 mg Pt/SiO$_2$ downstream.

[b] Estimated for reaction over Ni/SiO$_2$ alone at 140 °C. Values for alkanes and benzene are calculated using the vapour pressure data in Ref. [33] assuming that the vapour and liquid phases are fully equilibrated and Raoult's law is obeyed. Values for the unsaturates are estimated from that for the alkanes based on logarithmic interpolation against boiling points or, in cases where none was available, then against gas chromatographic retention time.

* See text.

umn resolution was sufficient to allow identification of many of the hydrogenation products formed by subsequent hydrogenation over Pt/SiO$_2$ (Fig. 8B). Table 4 lists the principal alkanes produced at 140 and 200 °C classified in the same way as in Table 1.

A particular difference arises in the classification of odd-numbered versus even-numbered products. Addition of C$_2$ to the second carbon of a linear C$_6$ intermediate would produce the backbone of 3-methylheptane and addition to the third carbon, that of 3-ethylhexane. Similarly C$_2$ addition to the second, third and fourth carbons of a linear C$_8$ could give rise to 3-methylnonane, 3-ethyloctane and 4-ethyloctane, respectively. The same 3- and 4-substituted hexanes, heptanes, octanes and nonanes could result if C$_2$ is added to the last carbon of the 3-substituted C$_6$ and C$_8$ intermediates. Formation of 5-methylnonane is also possible if C$_2$ is added to the first carbon of a C$_8$ surface species carrying a 3-methyl branch. Nonetheless the prohibition against formation of 2-methyl branched hydrogenation products remains regardless of chain length for even-numbered products.

Odd-numbered products are different in that the expected complete hydrogenation product following addition of a C$_2$ unit to the central carbon of a linear C$_3$ surface intermediate is 2-methylbutane. Higher 2-methyl products, 2-methylhexane, 2-methyloctane, etc. can then arise by further end-carbon addition. Unlike the situation for the 3-methyl and 3-ethyl substituted products (both even- and odd-numbered), 2-methylhexane, etc. cannot be formed by addition of C$_2$ to linear C$_5$, C$_7$, etc. surface species. Products that can only be formed from branched intermediates are denoted bI[*] in Table 4.

The product distribution in Table 4 conforms to that for C$_6$ products—linear alkanes were formed in the largest amounts followed by alkanes carrying a branch on the third carbon. Production of ethylcyclopentane (cC5) was approximately double that of toluene (cC6) and that of propylcyclopentane was twice that of ethylbenzene, similar to the relative amounts seen for methylcyclopentane versus benzene. The only xylene detected was o-xylene in a concentration much less than that of ethylbenzene. Regardless of carbon number, most alkanes were produced in higher yield at 140 °C than 200 °C, in accord with the greater hydrogenation effectiveness of Pt/SiO$_2$ at the lower temperature evident for C$_6$ compounds in Table 3. By contrast the yields of all aromatics increased with temperature.

In addition to the compounds listed in Table 4, the chromatogram in Fig. 8B shows many small peaks with retention times between 16.0 and 17.6 min. They could not be identified with certainty but fell in the range expected for the doubly branched C$_{10}$ products that could result from C$_2$ addition to internal carbons of already branched C$_8$ intermediates to yield, for example, the backbone of 3-methyl-5-ethylheptane.

The analytical results for the liquid phase in Table 4 can be combined with those for the vapour phase in Figs. 2 and 4 to ascertain the dependence of overall yield on carbon number. Fig. 9 shows this information for the reaction over Ni/SiO$_2$ plus Pt/SiO$_2$ at 140 °C plotted, for convenience, according to the logarithmic form of the Anderson–Schulz–Flory distribution [36]:

$$\log_{10} C_i = \log A + i \log_{10} \alpha$$

where C_i is the number of molecules of a product containing i units, α the chain growth probability (i.e. the probability of a surface species adding a C$_2$ unit versus conversion to a product molecule) and A is a constant. It should be recognised that the calculations here are of rather limited accuracy, since they rely heavily on the estimated collection efficiencies, and are also for alkanes alone, thus neglecting residual alkenes for which the concentration is structure dependent.
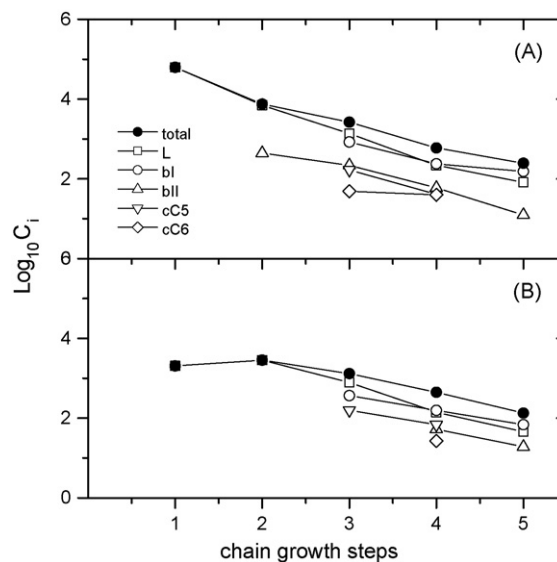

Fig. 9. Anderson–Schulz–Flory type plots of product distribution vs. the number of chain growth steps. (A) Products with an even number of carbon atoms; (B) products with an odd number of carbon atoms.

A plot for the even-numbered linear products taken together is reasonably linear (Fig. 9A). The apparent chain growth probability, calculated from the slope is 0.26. This is similar to the value for the Fischer–Tropsch synthesis using Ni/Al$_2$O$_3$ for which α ranges from 0.16 to 0.29 depending on the temperature and H$_2$/CO ratio [37]. Considering the classes separately, linear even-numbered alkanes have a lower apparent α value (0.22) than do branched ones (~0.4 for class bI). This is as one might expect qualitatively since the number of interior carbons increases relative to end carbons as the chain lengthens and branched surface species, once created, can only have branched daughters. Products with an odd number of carbons show a similar pattern (Fig. 9B) except that the concentration of the methane (shown at $i = 1$), is below the trend line for $i = 2, 3, 4$ and 5 (corresponding to molecules with 3, 5, 7 and 9 carbon atoms). Either C$_1$ starting species are terminated less efficiently than higher ones or propagation starts mainly from C$_3$ rather than C$_1$.

4. Discussion

The present findings add little to existing knowledge concerning the hydrogenation of acetylene to ethylene and ethane over nickel catalysts [38–41] and attention will be confined to routes to higher products. The low yield of aromatics found here is contrary to a recent report that benzene is the major C$_2$+ product when acetylene is hydrogenated over Ni/SiO$_2$ [17]. However it is broad agreement with the work of Sheridan [11] and of Antsus and Petrov [13] carried out before gas chromatography became available. Based on distillation and oxidation of individual fractions, the latter concluded that reaction over Ni/ZnCl$_2$/pumice produced largely branched and straight chain alkenes, exclusively even-numbered, plus some dienes and benzene. Octane determinations on fully hydrogenated fractions indicated that the branched/linear ratio was less than unity for C$_6$ compounds but greater than unity for C$_8$ products. The data of Sheridan were basically similar but with more evidence for odd-numbered molecules, less for formation of isoalkenes, especially isobutene, and none for dienes or aromatics [11].

While construction of carbon backbone of the two major product classes, linear and branched I, is easily envisaged in the way described earlier, the number of hydrogen atoms carried by each carbon in surface species during construction is problematic. The

original suggestion of Sheridan [11], extended in the book by Bond [42], was that hydrogenation of diadsorbed acetylene molecules produced a half-hydrogenated state that had a radical form, i.e.

$$HC^*{=}C^*H + H^* \rightarrow H_2C{=}C^*H \rightarrow H_2C^*{-}{^\bullet}C^*H$$
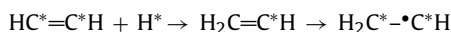
where '*' represents binding to a surface site. Addition of diadsorbed acetylene to the radical would then give a C_4 radical:

$$H_2C^*{-}{^\bullet}C^*H + HC^*{=}C^*H \rightarrow H_2C^*{-}C^*H{-}C^*H{=}{^\bullet}C^*H, \quad etc.$$

and with further chain growth, linear C_6, C_8, etc. products.

This scheme does not allow for branched products. The suggestion made was that the radical and normal half-hydrogenated states combined to form a secondary butyl radical:

$$H_2C^*{-}{^\bullet}C^*H + H_2C{=}C^*H \rightarrow H_2C^*{-}C^*H{-}{^\bullet}CH{-}C^*H_2$$
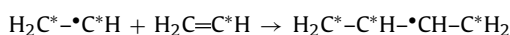
to which diadsorbed acetylene could add to form an intermediate with the carbon backbone arrangement of 3-methylpentane. A problem with this scheme is that since all carbons bound to the surface carry hydrogen atoms initially, hydrogenation of surface links could not produce compounds without hydrogen atoms at the branch. This is contrary to the experimental finding that the branched C_6 dienes formed in the largest amounts, cis- and trans-3-methyl-1,3-pentadiene:
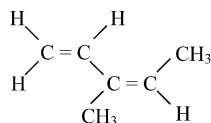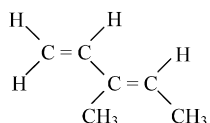
cis–3-methyl-1,3-pentadiene   trans–3-methyl-1,3-pentadiene

have that arrangement and it is preserved in the products of hydrogenation of their terminal double bonds, cis- and trans-3-methyl-2-pentene (numbering from the opposite end). A further C_6 alkene product, 2-ethyl-1-butene, also has a carbon lacking a hydrogen atom.

There is little direct evidence for the existence of the radical species in Sheridan's scheme. Surface science studies, backed by calculations, show that acetylene adsorbs non-dissociatively on Ni(1 1 1) at 120 K in a μ-bridge (di-σ/di-π) form in which the CC bond lies across adjoining Ni–Ni atom pairs with binding to four Ni atoms [43,44]. The bond length matches the 144 pm distance between surface hollows, corresponding to a hybridisation between sp^2 and sp^3. This electronic arrangement is supported by vibrational studies of acetylene adsorbed on both Ni(1 1 1) and Ni(1 0 0) but the species present on Ni(1 1 0) are probably di-σ/π bonded [45–48]. Dissociation to acetylide (–C≡CH) and/or methylidyne (≡C–H) species, and then to carbon sets in at higher temperatures [49–51], but the species are not well defined [48,49]. Onset temperatures as low as 190 K have been reported for the dissociation of acetylene on stepped nickel surfaces [45] but ambient temperatures and above are more usual for dissociation on low-index planes [45,47,50,51]. The best documented hydrogenated surface species is ethylidyne (CH₃C≡), which can be formed on Ni(1 1 1) by the reaction of surface, bulk or gas phase H atoms with adsorbed acetylene at sub-ambient temperatures [52,53]. Vinyl species (CH₂=CH–) are thought to be intermediates in the process but are too reactive to be observed directly.

Based on the established species, the simplest scheme for oligomerization is one in which a reactive vinyl species acts as an initiator for addition of di-σ/di-π surface C_2H_2 species, i.e.
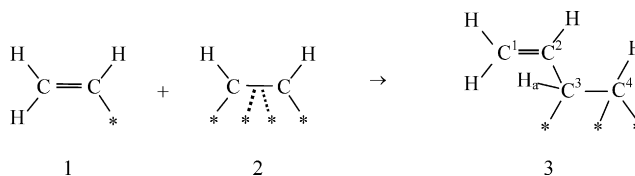
Hydrogenation of the surface links in 3 would be expected to produce 1-butene or 1,3-butadiene, depending on the availability of surface hydrogen, with formation of cis- and trans-2-butenes also possible if the double bond opened and was followed by 1,4 hydrogen addition. Linear hexenes, hexadienes and hexatriene could arise in a similar fashion if the chain was lengthened through addition of another C_2H_2 surface species to carbon 4.

If another C_2H_2 surface species were to add to carbon 3 of species 3:
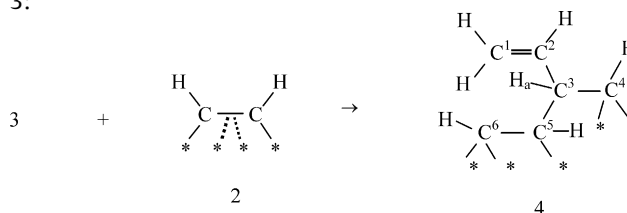
then the monoalkene product expected on hydrogenation of all links to the surface in 4 would be 3-methyl-1-pentene, which is indeed a substantial C_6 product (Fig. 7A). However, cis- and trans-3-methyl-2-pentene and 2-ethyl-1-butene, the other three major branched C_6 alkene products, could not be formed directly.

A possible explanation is as follows. The only diene that could be formed directly from 4 (by addition of two hydrogen atoms to carbon 4 and one to carbon 6) is 3-methyl-1,4-pentadiene. This is by far the least stable methylpentadiene, because the double bonds are not conjugated, and was barely detectable as a product (in Fig. 6A with a retention time of 4.47 min). Isomerization to other more stable methylpentadienes and their hydrogenation is thus a possible route to the above three alkenes. The finding that the trans/cis ratio is greater than unity in the 3-methyl-2-pentenes (i.e. as expected for equilibrium), which is not the case with the linear hexenes, is consistent with the presence of a secondary reaction.

Alternatively, species 4 might rearrange to another surface species capable of producing conjugated products. This requires detachment of the hydrogen from carbon 3 (i.e. H_a), possibly facilitated if the stereochemistry forming species 4 directed H_a towards the surface, and/or this was aided by hydrogenation of the surface links to other carbons. For example, if carbons 4 and 6 were hydrogenated, then detachment of H_a would allow formation of a double bond between carbons 3 and 5 with liberation of cis/trans-3-methyl-1,3-pentadiene (the C_6 dienes observed in largest quantities). Opening of the C_1 to C_2 double bond would then give the cis- and trans-3-methyl-2-pentenes. Likewise hydrogenation at carbons 5 and 6 and detachment of H_a would allow creation of a double bond between carbons 3 and 4 and formation of the observed 2-ethyl-1-butene if the carbon 1 to carbon 2 double bond was opened.

Further addition of C_2H_2 units may be subject to restrictions arising from the strain that would accumulate as more carbon atoms beyond the vinyl group were bound to the surface. This is particularly the case in linear intermediates where, unlike the situation in species 4, all carbon atoms are bound to the surface, e.g.
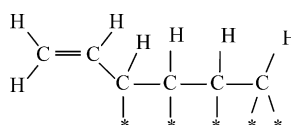
The strain could be relieved in three ways—hydrogenation of carbon to surface bonds, combination of adjacent carbon to surface bonds to form a polyene chain, or fragmentation at some point in the bound section. Division into two chains, potentially with an odd number of carbon atoms that grow by C_2H_2 addition, would account for the substantial fraction of the final products being of that type. The alternative, that odd-numbered products were derived by growth from C1 species seems less likely under the conditions used here given that the yield of methane was much less than that of either C_3 or C_5 products.

Concerning minor products, the formation of cyclic five- and six-membered ring compounds is readily envisaged. If linear intermediates with 5 or more carbon atoms are arranged *cis–cis* on a metal surface then the first and fifth or sixth carbons become close enough to permit linkage. *cis*-1,3,5-Hexatriene, traces of which are evident in Fig. 7A, undergoes cyclization rather readily, in the gas phase to cyclo-1,3-hexadiene [54], to mixtures of cyclic C_6 and methyl-substituted C_5 compounds on various oxides including silica gel [55] and, via dehydrogenation, to benzene on Pt black [56] and on $Cu_3Pt(1\,1\,1)$ surfaces [57,58]. There is no information for nickel-containing systems.

The route to the unexpected branched products of type bII (i.e. even-numbered ones with a 2-methyl branch) is not so obvious. They are present at concentrations typically around one-quarter their 3-methyl counterparts with isobutene, in particular, accounting for ∼2% of the acetylene fed (Fig. 4). Interconversion between 2- and 3-methylpentanes is well known during naphtha reforming over platinum-based catalysts but requires temperatures in excess of 350 °C. The usual activity order on metals is *cis–trans* isomerisation > double bond shift > hydrogenation > dehydrogenation > skeletal isomerisation. Since the *cis*-2/*trans*-2 and 1-/2-isomer distributions amongst linear oligomers are far from equilibrium during oligomerization, it appears highly likely that type bII products are primary reaction products rather than the result of rearrangements.

The simplest explanation, contained in the old work of Antsus and Petrov [13], is that 2-methyl compounds arise through formation of a transient three-membered ring intermediate, e.g.
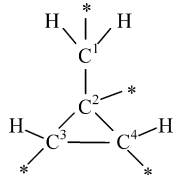
Rupture of the 3–4 bond followed by partial hydrogenation or chain growth could then give rise to isobutene and higher 2-methyl compounds.

The schemes above are speculative but the complex nature of the product distribution, with formation of unexpected products, indicates a multitude of pathways.

5. Conclusions

Under the standard test conditions used here, a low-loaded nickel on silica catalyst is capable of the complete conversion of acetylene in the presence of hydrogen with oligomers accounting for close to one-half of the acetylene reacted. The mixture of oligomers is highly complex but can be simplified by hydrogenation to alkanes over a Pt/SiO_2 catalyst placed downstream. Even though methane is a minor product, the product spectrum includes many higher compounds with an odd number of carbon atoms, each in amounts about one-half of that of the succeeding even-numbered ones. The two largest product classes are linear alkenes with a non-equilibrium distribution (1->*cis*->*trans*-) and 3-methyl branched alkenes that can, in principle, arise through addition of a C_2 surface intermediate to a linear precursor. However the reaction also produces some 2-methyl-branched compounds that cannot arise that way. Other minor products include possible diene progenitors for some alkenes and unsaturated five-membered rings molecules that give rise to cyclopentanes when hydrogenated on Pt/SiO_2. Contrary to some data in the literature, aromatics are very minor products when Ni/SiO_2 is used under the present conditions. A majority of the branched-chain alkene products lack hydrogen atoms at the branch, consistent with isomerization of an unstable diene primary product or surface rearrangements involving hydrogen abstraction. The formation of all major product classes, with the exception of those with a 2-methyl branch, can be rationalised in terms of growth from surface species established by surface science studies of the interaction of acetylene with various nickel surfaces.

Under the present standard conditions, deactivation was not observable over an initial period of 5 h at 140 °C and proceeded slowly thereafter. The rate of deactivation increased substantially at higher temperature and was also faster if the concentration of acetylene in the feed was increased relative to that of hydrogen.

References

[1] K.R. Hall, A. Akgerman, R.G. Anthony, P.T. Eubank, J.A. Bullin, J.G. Cantrell, B.R. Weber, J. Betsill, APPEA J. (2002) 59.
[2] K.R. Hall, Catal. Today 106 (2005) 243.
[3] K.R. Hall, J.A. Bullin, P.T. Eubank, A. Akgerman, R.G. Anthony, United States Patent 6,323,247 (2001).
[4] K.R. Hall, J.A. Bullin, P.T. Eubank, A. Akgerman, R.G. Anthony, United States Patent 6,130,260 (2000).
[5] K.R. Hall, J.A. Bullin, P.T. Eubank, A. Akgerman, R.G. Anthony, United States Patent 6,602,920 (2003).
[6] A. Alkhawaldeh, X. Wu, R.G. Anthony, Catal. Today 84 (2003) 43.
[7] P. Tsai, J.R. Anderson, J. Catal. 80 (1983) 207.
[8] Y. He, W.-L. Jang, R.B. Timmons, Energy Fuels 5 (1991) 613.
[9] Y. He, W.-L. Jang, R.B. Timmons, ACS Symp. Ser. 517 (1993) 355.
[10] K. Peters, L. Neumann, Ges. Abhandl. Kenntnis Kohle 11 (1932) 423.
[11] J. Sheridan, J. Chem. Soc. (1945) 133.
[12] A.D. Petrov, L.I. Antsus, Dokl. Akad. Nauk SSSR, Ser. A 4 (1934) 300.
[13] L.I. Antsus, A.D. Petrov, Petrol. Refiner. 23 (1944) 317.
[14] L.I. Antsus, A.D. Petrov, Dokl. Akad. Nauk SSSR, Ser. A 53 (1946) 619.
[15] A.D. Petrov, L.I. Antsus, M.A. Cheltsova, Izv. Akad. Nauk SSSR, Ser. Khim. (1947) 363.
[16] S. Vasquez, PhD Thesis, University of Texas at Arlington, 1997.
[17] A.-G. Boudjahem, S. Monteverdi, M. Mercy, M.M. Bettahar, Appl. Catal. A: Gen. 250 (2003) 49.
[18] D. Trimm, I. Liu, N. Cant, Stud. Surf. Sci. Catal. 172 (2007) 309.
[19] ASTM Standard Test Method D6730-01: Determination of Individual Components in Spark Ignition Engine Fuels by 100-m Capillary (with Precolumn) High Resolution Gas Chromatography, ASTM International, West Conshohocken, 2002.
[20] L. Sojak, G. Addova, R. Kubinec, A. Kraus, G. Hu, J. Chromatogr. A 947 (2002) 103.
[21] L. Sojak, G. Addova, R. Kubinec, A. Kraus, A. Bohac, J. Chromatogr. A 1025 (2004) 237.
[22] P.C. Hayes, E.W. Pitzer, J. High Res. Chromatogr. 8 (1985) 230.
[23] S.E. Stein, in: P.J. Linstrom, W.G. Mallard (Eds.), NIST Chemistry WebBook, NIST Standard Reference Database Number 69, National Institute of Standards, Gaithersburg, MD 20899, June, 2005.
[24] M.I. Altbach, C.P. Fitzpatrick, Fuel 73 (1994) 223.
[25] B. Mile, D. Stirling, M.A. Zammitt, A. Lovell, M. Webb, J. Catal. 114 (1988) 217.
[26] K. Hadjiivanov, M. Mihaylov, D. Klissurski, P. Stefanov, N. Abadjieva, E. Vassileva, L. Mintchev, J. Catal. 185 (1999) 314.
[27] S. Tomiyama, R. Takahashi, S. Sato, T. Sodesawa, S. Yoshida, Appl. Catal. A: Gen. 241 (2003) 349.

[28] G.C. Bond, Metal-Catalysed Reactions of Hydrocarbons, Springer, New York, 2005.

[29] E.F. Meyer, D.G. Stroz, J. Am. Chem. Soc. 94 (1972) 6344.

[30] R.G. Oliver, P.B. Wells, J. Grant, in: J.W. Hightower (Ed.), Proceedings of the Fifth International Congress on Catalysis, vol. 1, Miami, 1972, pp. 659–667.

[31] R.A. Ross, G.D. Martin, W.G. Cook, Ind. Eng. Chem. Prod. Res. Dev. 14 (1975) 151.

[32] R.H. Ewell, P.E. Hardy, J. Am. Chem. Soc. 63 (1941) 3460.

[33] R.C. Weast, Handbook of Chemistry and Physics, The Chemical Rubber Company, Cleveland, 1970.

[34] J.E. Kilpatrick, E.J. Prosen, K.S. Pitzer, F.D. Rossini, J. Res. Nat. Bur. Stand. 36 (1946) 559.

[35] S.E. Stein, R.L. Brown, in: P.J. Linstrom, W.G. Mallard (Eds.), NIST Standard Reference Database Number 69, National Institute of Standards, Gaithersburg, MD 20899, June, 2005.

[36] R.J. Farrauto, C.H. Bartholomew, Fundamentals of Industrial Catalytic Processes, Blackie, London, 1997.

[37] D.M. Stockwell, C.O. Bennett, J. Catal. 110 (1988) 354.

[38] G.C. Bond, J. Chem. Soc. (1958) 2705.

[39] G.C. Bond, J. Chem. Soc. (1958) 4288.

[40] G.C. Bond, R.S. Mann, J. Chem. Soc. (1958) 4738.

[41] G.F. Berndt, S.J. Thomson, G. Webb, J. Chem. Soc., Faraday Trans. I 79 (1983) 195.

[42] G.C. Bond, Catalysis by Metals, Academic Press, London, 1962.

[43] S. Bao, P. Hofmann, K.-M. Schindler, V. Fritzsche, A.M. Bradshaw, D.P. Woodruff, C. Casado, M.C. Asencio, Surf. Sci. 307–309 (1994) 722.

[44] J.W. Medlin, M.D. Allendorf, J. Phys. Chem. B 107 (2003) 217.

[45] S. Lehwald, H. Ibach, Surf. Sci. 89 (1979) 425.

[46] J.A. Stroscio, S.R. Bare, W. Ho, Surf. Sci. 148 (1984) 499.

[47] F. Zaera, R.B. Hall, J. Phys. Chem. 91 (1987) 4318.

[48] N. Sheppard, C. De La Cruz, Adv. Catal. 42 (1998) 181.

[49] A. Morgante, S. Modesti, M. Bertolo, P. Rudolf, R. Rosei, Surf. Sci. 211–212 (1989) 829.

[50] M. Weinelt, W. Huber, P. Zebisch, H.-P. Steinruck, P. Ulbright, U. Birkenheuer, J.C. Boettger, N. Rosch, J. Chem. Phys. 102 (1995) 9709.

[51] R. Neubauer, C.M. Whelan, R. Denecke, H.-P. Steinruck, J. Chem. Phys. 119 (2003) 1710.

[52] K.L. Haug, T. Burgi, M. Gostein, T.R. Trautmann, S.T. Ceyer, J. Phys. Chem. B 105 (2001) 11480.

[53] T. Burgi, T.R. Trautmann, M. Gostein, D.L. Lahr, K.L. Haug, S.T. Ceyer, Surf. Sci. 501 (2002) 49.

[54] K.E. Lewis, H. Steiner, J. Chem. Soc. (1963) 3080.

[55] B.A. Kazanskii, M.I. Rozengart, V.L. Polinin, V.G. Bryukhanov, L.V. Kravtsova, N.I. Kolpakova, Russ. Chem. Bull. 25 (1976) 1685.

[56] Z. Paal, P. Tetenyi, J. Catal. 30 (1973) 350.

[57] A.V. Teplyakov, B.E. Bent, J. Phys. Chem. B 101 (1997) 9052.

[58] A.V. Teplyakov, A.B. Gurevich, E.R. Garland, B.E. Bent, Langmuir 14 (1998) 1337.